Structure, Vol. 10, 1291–1301, October, 2003, ©2003 Elsevier Science Ltd. All rights reserved. DOI 10.1016/j.str.2003.09.006

Structure and Interactions of NCAM Ig1-2-3 Suggest a Novel Zipper Mechanism for Homophilic Adhesion

Vladislav Soroka,[1] Kateryna Kolkova,[1] Jette S. Kastrup,[2,*] Kay Diederichs,[3] Jason Breed,[3] Vladislav V. Kiselyov,[1] Flemming M. Poulsen,[4] Ingrid K. Larsen,[2] Wolfram Welte,[3] Vladimir Berezin,[1] Elisabeth Bock,[1] and Christina Kasper[2]

[1]Protein Laboratory
Institute of Molecular Pathology
Panum Institute
Blegdamsvej 3 C
DK-2200 Copenhagen
Denmark

[2]Department of Medicinal Chemistry
Danish University of Pharmaceutical Sciences
Universitetsparken 2
DK-2100 Copenhagen
Denmark

[3]Department of Biology
University of Konstanz
Universitätsstraße 10
D-78464 Konstanz
Germany

[4]Institute of Molecular Biology
University of Copenhagen
Øster Farimagsgade 2A
DK-1353 Copenhagen
Denmark

Summary

The neural cell adhesion molecule, NCAM, mediates Ca^{2+}-independent cell-cell and cell-substratum adhesion via homophilic (NCAM-NCAM) and heterophilic (NCAM-non-NCAM molecules) binding. NCAM plays a key role in neural development, regeneration, and synaptic plasticity, including learning and memory consolidation. The crystal structure of a fragment comprising the three N-terminal Ig modules of rat NCAM has been determined to 2.0 Å resolution. Based on crystallographic data and biological experiments we present a novel model for NCAM homophilic binding. The Ig1 and Ig2 modules mediate dimerization of NCAM molecules situated on the same cell surface (*cis* interactions), whereas the Ig3 module mediates interactions between NCAM molecules expressed on the surface of opposing cells (*trans* interactions) through simultaneous binding to the Ig1 and Ig2 modules. This arrangement results in two perpendicular zippers forming a double zipper-like NCAM adhesion complex.

Introduction

It is crucial for the development and maintenance of cells and tissues that external cues can induce fast and appropriate responses at the cellular level. Interactions between cells and between cells and components of the surrounding extracellular matrix are important in this respect. Therefore, extensive studies have been performed to elucidate the mechanisms of homophilic and heterophilic interactions mediated by cell-cell adhesion molecules (CAMs) (Chothia and Jones, 1997).

The neural cell adhesion molecule, NCAM, mediates adhesion of cells to other cells as well as to components of the extracellular matrix. At the molecular level, NCAM binding has been shown to activate intracellular signaling cascades that lead to cellular responses such as differentiation, growth, survival, and modulation of neuronal connections in association with regenerative and cognitive processes (Covault and Sanes, 1985; Tomasiewicz et al., 1993; Berezin et al., 2000). NCAM is consequently a protein of great biological interest.

NCAM belongs to the immunoglobulin (Ig) superfamily and mediates Ca^{2+}-independent cell-cell and cell-substratum adhesion via homophilic and heterophilic interactions. Alternative splicing of mRNA generates three major NCAM isoforms; those extracellular parts consist of five N-terminal Ig modules followed by two fibronectin type III modules (Cunningham et al., 1987). The different modules of NCAM have been shown to perform distinct functions (Probstmeier et al., 1989; Kasper et al., 1996; Kiselyov et al., 1997). NCAM binds various extracellular matrix components such as heparin/heparan sulfate (Nybroe et al., 1989; Kallapur and Akeson, 1992), chondroitin sulfate proteoglycans (Milev et al., 1994), and different types of collagen (Probstmeier et al., 1989; Kiselyov et al., 1997). The heparin binding sequence is localized to the Ig2 module (Cole and Akeson, 1989). Despite extensive studies, the precise mechanism of the homophilic binding of NCAM remains unclear, and the published results are to some extent contradictory. At least two groups of researchers suggest that recombinant chicken Ig3 produced in *E. coli* can self-associate (Rao et al., 1992; Ranheim et al., 1996). A binding has also been demonstrated between recombinant modules Ig1 and Ig5 and between Ig2 and Ig4 in chicken NCAM, as well as between modules Ig1 and Ig2 in rat and chicken NCAM (Ranheim et al., 1996; Kiselyov et al., 1997; Jensen et al., 1999; Atkins et al., 1999).

The three-dimensional structures of individual modules of rat Ig1 and Ig2, and the chicken Ig1 and Ig3 modules, have been determined by nuclear magnetic resonance (NMR) spectroscopy, resulting in the identification of amino acid residues involved in the homophilic binding between the Ig1 and Ig2 modules (Jensen et al., 1999; Atkins et al., 1999). The crystal structure of the Ig1-2 fragment of rat NCAM provided detailed information on the crosslike Ig1-2 dimer and pointed out the key residues in this interaction, namely Phe19 and Tyr65 (Kasper et al., 2000). In contrast with earlier findings, recent experiments did not reveal any self-association of chicken Ig3, even though the Ig3 module was folded and clearly inhibited aggregation of synthetic lipid vesicles containing NCAM (Atkins et al., 2001). Moreover, the same group has demonstrated that a point mutation F19S did not affect cell aggregation mediated by full-

*Correspondence: jsk@dfh.dk

Table 1. Crystallographic Data and Refinement Statistics

	Native Data Set
Wavelength (Å)	1.0526
Resolution range (Å)[1]	50.0-2.0 (2.07-2.0)
Number of observed reflections	164,206
Number of unique reflections	27,881
Number of reflections in R_{free} set	828
Completeness (%)	99.2 (99.4)
$I/\sigma(I)$	19.6 (1.4)
(R_{merge}) (%)[2]	3.9 (20.9)
R_{cryst}/R_{free} (%)[3]	21.8/23.8
Number of refined non-hydrogen atoms[4]	
Protein	2248
Water	265
Average B-factor (all atoms, Å^2)	60
Wilson B-factor (Å^2)	45
R.m.s. Δ bond lengths/angles[5]	0.0081/1.7
Residues in allowed regions (%)[6]	97%

[1] Values in parentheses are statistics for the highest resolution bin.
[2] $R_{merge}(I) = \Sigma_{hkl}|I_{hkl} - <I_{hkl}>|/\Sigma_{hkl}I_{hkl}$, where I_{hkl} is the measured intensity of the reflections with indices *hkl*.
[3] $R = \Sigma_{hkl}||Fo| - |Fc||/\Sigma|Fo|$, are the observed and calculated structure factor amplitudes for reflection hkl, applied to the work (R_{cryst} = 97%) and test (R_{free} = 3%) sets, respectively.
[4] Residues −2, 239, and 240 were not located. Residues originating from the cloning site were given negative integers.
[5] Root mean squared deviations (rms Δ) in bond length and angles from ideal values.
[6] The Ramachandran plot was calculated according to Kleywegt and Jones (1996).

length NCAM, even though it abolished dimerization of the Ig1-2-3 fragment in solution. These results therefore question the suggested Ig3-to-Ig3 (Rao et al., 1992; Ranheim et al., 1996) and Ig1-to-Ig2 (Kiselyov et al., 1997; Kasper et al., 2000) models of NCAM homophilic binding. The controversy with respect to the molecular mechanism of NCAM-mediated homophilic binding, and numerous results implying a key role of the Ig3 module, encouraged us to determine the X-ray structure of the Ig1-2-3 fragment of rat NCAM. Here, we report the 2.0 Å X-ray structure of this fragment, which discloses the importance of all three modules for homophilic binding. Based on the structure and on results from cell culture experiments using selected Ig3 module mutants and peptides derived from the NCAM sequence, a novel model for the mechanism of NCAM-mediated homophilic adhesion is presented.

Results and Discussion

The X-Ray Structure of the Ig1-2-3 Modules of NCAM

The X-ray structure of NCAM Ig1-2-3 was determined to 2.0 Å resolution (Table 1). In the structure of Ig1-2-3, the Ig1 and Ig2 modules are positioned in an extended conformation with Ig3 oriented at an angle of approximately 45° to the Ig1-Ig2 axis (Figure 1). The linker regions between Ig1-Ig2 and between Ig2-Ig3 are short and comprise only two (Lys98-Leu99) and one (Asn190) residues, respectively. The overall structure of the Ig1 and Ig2 modules is very similar to the previously determined Ig1-2 structure (Kasper et al., 2000) with root mean square deviations (r.m.s.d.) of 0.7 (96 Cα atoms) and 0.8 Å (93 Cα atoms), respectively. In the Ig1-2-3 structure, the tilt angle between Ig1 and Ig2 is 11° and thereby differs by 13° compared to the Ig1-2 structure.

The 98-residue Ig3 module of rat NCAM adopts the topology of an intermediate type 1 (I1) set Ig module (Casasnovas et al., 1998). In the Ig3 module, the classical β sandwich consists of two β sheets with a total of nine β-strands (Figure 1B). The A, B, D, and E β-strands make up one sheet and the A′, C, C′, F, and G β- strands the second sheet. A cysteine bridge Cys216-Cys269 connects the two β sheets. All strands are antiparallel except for the A′-strand, which runs parallel to the C-terminal part of the G-strand. Ig3 contains one site for N-linked glycosylation at Asn203 positioned in the A′-strand. The E-F-loop (residues Lys261-Asp263) forms a 3_{10} α-helical turn. The overall structure of rat Ig3 is similar to the structure of chicken Ig3 (Atkins et al., 2001) with r.m.s.d. of 1.65 Å (95 Cα atoms).

Parallel Interactions between Ig Modules

Several characteristic interactions are observed in the structure of the NCAM Ig1-2-3 fragment, which may be divided into two groups: interactions where the long axes (N to C terminus) of two interacting Ig1-2-3 molecules are oriented in a parallel manner and interactions where the long axes are oriented in an antiparallel manner. One parallel interaction and three major antiparallel interactions are observed in the crystal.

The parallel, crosslike dimer interaction of NCAM Ig1-2-3 involves the Ig1 and Ig2 modules (Figure 2). The total buried surface area of this interface is 1594 Å^2 (per dimer), which is similar to that previously observed in the Ig1-2 crosslike dimers (Kasper et al., 2000). The most prominent feature of the Ig1-to-Ig2 interaction is the intercalation of two aromatic residues of Ig1, Phe19 and Tyr65, into hydrophobic pockets formed by Ig2 residues (Figure 3A), which was also observed in the Ig1-2 structure. However, a tighter Ig1 to Ig2 binding interface is observed in the Ig1-2-3 structure, where the hydroxyl group of Tyr65 forms a direct hydrogen bond (H-bond) with Glu171, instead of a water-mediated H-bond as observed in Ig1-2. Tyr65 also makes three H-bonds to the side chains of Lys133, Glu171, and Arg173. Arg173 forms part of the Ig2 hydrophobic pocket and makes two H-bonds to Thr63. The parallel orientation of the Arg173 and Phe19 side chains and the distance between the Nη1 atom of the guanidinium group of Arg173 and the Cζ atom of the benzene ring of Phe19 (3.4 Å) suggest a cation-π interaction between these two residues (Flocco and Mowbray, 1994).

Dynamic light scattering (DLS) measurements showed that deglycosylated Ig1-2-3 forms a single species of molecules in solution with a molecular weight of ~78 kDa, corresponding to a dimer. In order to demonstrate that Ig1-2-3 dimerization is mediated by the observed Ig1 to Ig2 binding, we produced a mutant of Ig1-2-3 (Ig1-2-3mut) containing three Ala substitutions: E11A, E16A, and K18A. These mutations have previously been shown to completely abolish dimerization of the Ig1-2 NCAM fragment in solution (Jensen et al., 1999). In the present structure Glu11 and Glu16 form intramolecular salt bridges, respectively, with Arg177 and Lys98 from

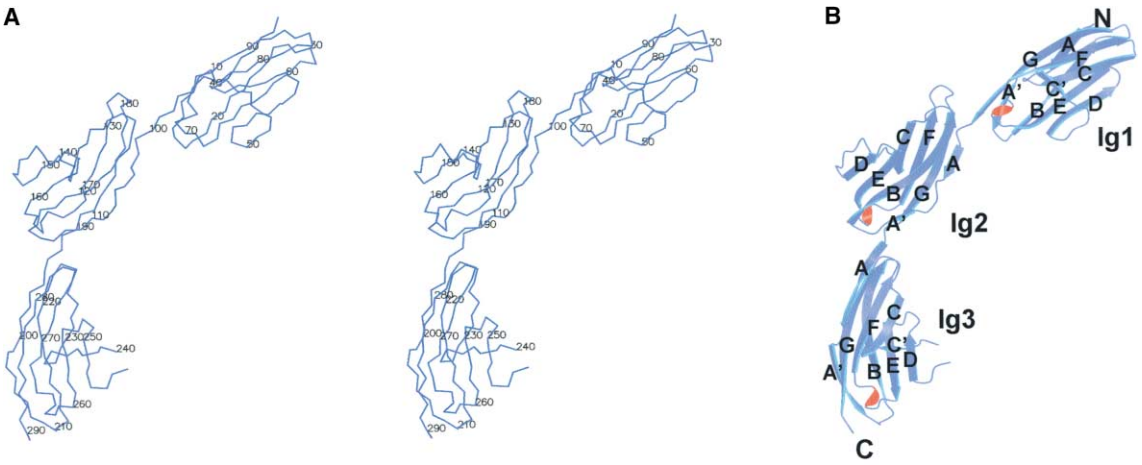

Figure 1. Crystal Structure of the Rat NCAM Ig1-2-3 Fragment at 2.0 Å Resolution

(A) Cα backbone diagram in stereo with every tenth residue labeled.

(B) Ribbon diagram with β-strands shown in blue and labeled according to Ig I set nomenclature. The $\alpha 3_{10}$ turns are shown in red.

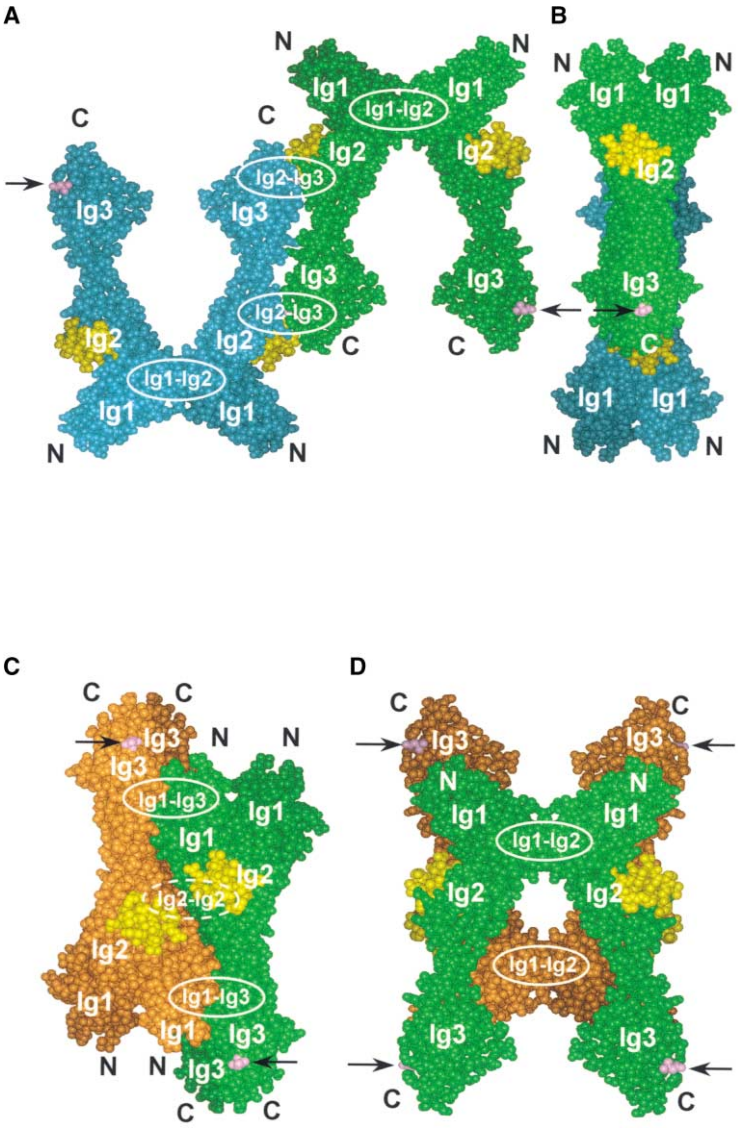

Figure 2. Crystal Structure of the Ig1-2-3 Fragment of NCAM Reveals Four Major Module-Module Interactions and Two Kinds of Ig1-2-3 Arrays

Space-filling models of interacting Ig1-2-3 *cis* dimers (mediated by Ig1-Ig2 binding) are shown. The Ig1-to-Ig2, Ig1-to-Ig3, Ig2-to-Ig2, and Ig2-to-Ig3 interaction sites are indicated by white ellipses. The heparin binding sites of the Ig2 modules (residues 133-148) are shown in yellow. The arrows indicate the position of N-linked glycosylation at Asn203 (Asn203 is colored pink). The termini are denoted by N and C.

(A and B) The Ig1-2 mediated *cis* dimers of the Ig1-2-3 fragment are shown in cyan and green and form a flat zipper via an Ig2-to-Ig3 mediated *trans* interaction, reflecting an interaction between NCAM molecules on opposing cells.

(C and D) The Ig1-2-3 fragment *cis* dimers also form a nonsymmetrical compact zipper via Ig1-to-Ig3 and Ig2-to-Ig2 *trans* interactions. Two *cis* dimers shown in orange and green are held together by two Ig1-to-Ig3 interactions (full ellipses) on one side and one Ig2-to-Ig2 interaction (stippled ellipse) on the opposite side of the zipper. The views in (B) and (D) are perpendicular to (A) and (C), respectively.

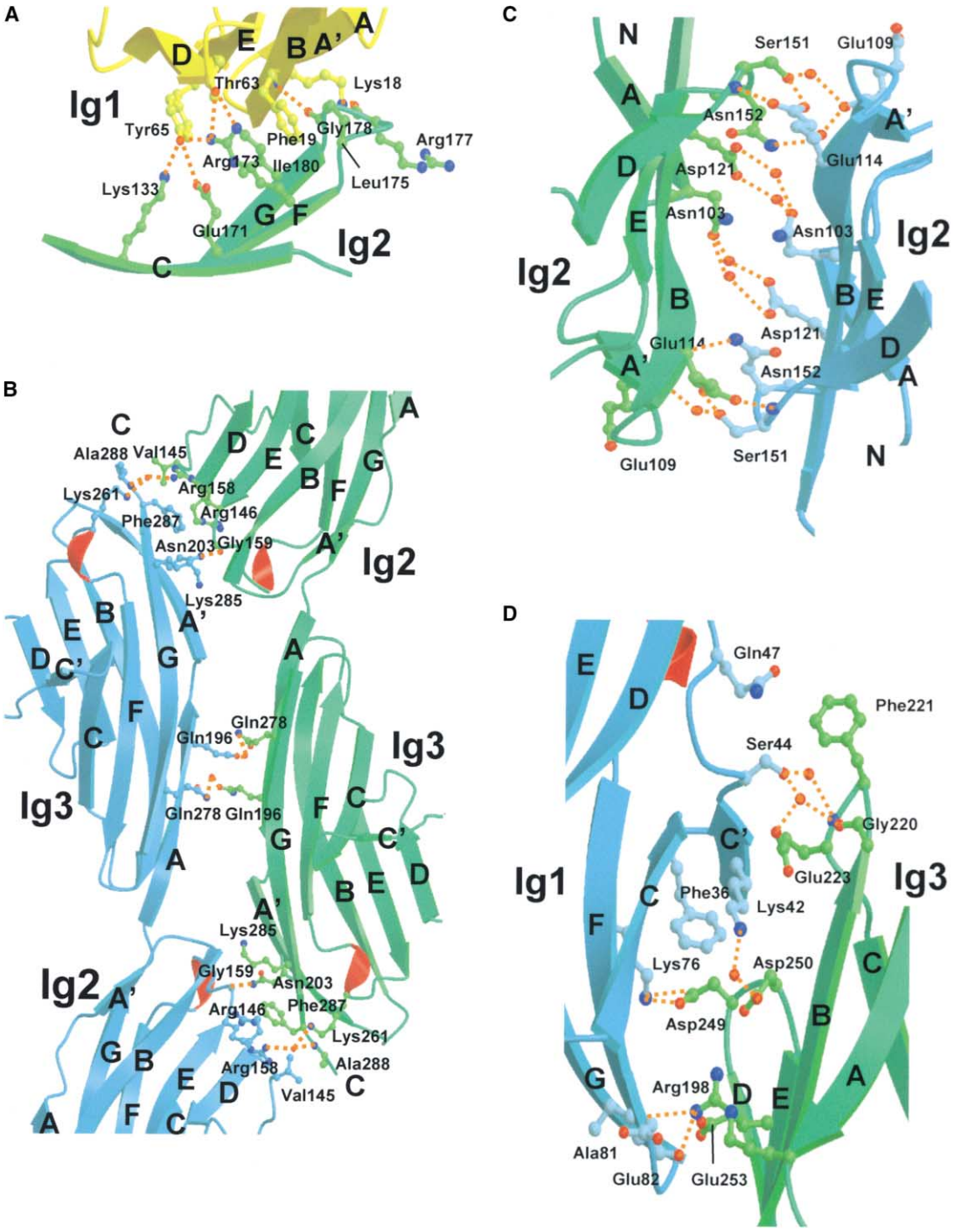

Figure 3. Closeup View of the Interaction Interfaces in the NCAM Ig1-2-3 Fragment

(A) The Ig1-to-Ig2 interaction interface. The Ig1 and Ig2 modules are shown in yellow and green and belong to two different Ig1-2-3 fragments that form one Ig1-2-3 *cis* dimer.

(B) The Ig2-to-Ig3 interaction interface.

(C) The Ig2-to-Ig2 interaction interface.

(D) The Ig1-to-Ig3 interaction interface.

In (B)–(D), the ribbon representations of modules from two interacting Ig1-2-3 fragments belonging to different Ig1-2-3 *cis* dimers are shown in green and cyan. Oxygen atoms are shown in red and nitrogens in blue. The hydrogen bonds are shown as red dashed lines. Water molecules are shown as red spheres.

the Ig1 to Ig2 linker region (not shown). These salt bridges probably contribute to the proper orientation of Ig1 with respect to Ig2 and therefore are important for the Ig1-to-Ig2 interaction. Lys18 forms an H-bond with the carboxyl group of Arg177 from the Ig2 module stabilizing the Ig1-Ig2 interaction (Figure 3A). Lys18 is located near

Phe19, which is the critical residue for the Ig1-to-Ig2 interaction as it was clearly demonstrated earlier (Atkins et al., 2001). Therefore, disruption of the Lys18-Arg177 H-bond may affect the orientation of Phe19, leading to elimination of the Ig1-to-Ig2 interaction. The molecular weight of the Ig1-2-3mut fragment was determined by DLS to be ~34 kDa, indicating a monomer. This confirms that Ig1-2-3 dimerization is mediated by Ig1-to-Ig2 binding.

Parallel (*cis*) interactions are not uncommon among cell adhesion molecules. Thus, *cis* dimerization has been demonstrated for the cell adhesion molecules C-CAM1, C-CAM2, ICAM-1, nectin-2α, and JAM belonging to the Ig superfamily (Hunter et al., 1996; Casasnovas et al., 1998; Miyahara et al., 2000; Kostrewa et al., 2001) as well as for N-, E-, and C-cadherins (Shapiro et al., 1995; Takeda et al., 1999; Brieher et al., 1996). It was shown that the dimeric form of C-cadherin is capable of adhesion, whereas the monomeric form is not (Brieher et al., 1996).

Antiparallel Interactions between Ig Modules

An antiparallel interaction takes place between the Ig2 and Ig3 modules of two Ig1-2-3 molecules, thereby forming arrays of Ig1-2-3 dimers (Figures 2A and 2B). Ig2 of one molecule binds to Ig3 of a second molecule, and vice versa (Figure 3B). The residues involved are 112-115, 143-146, and 158-161 from the B-strand, CD-loop/D-strand, and E-strand of Ig2, and residues 200-205, 261, and 278-289 from the A′-strand, EF-loop, and G-strand of Ig3. A central element of this interaction is the intercalation of the side chain of Phe287 from Ig3 into a hydrophobic pocket formed by the side chains of Val145, Arg146, and Arg158 of the Ig2 module and Lys285 from Ig3. Arg158 is also involved in water-mediated hydrogen bonding to residues Lys261 and Ala288, and Gly159 makes a direct H-bond to Asn203.

The crystal packing leaves room for glycosylation at Asn203. In order to accommodate N-linked glycosylation at this site, the side chain of Asn203 has to adopt another rotamer conformation. Thereby, the carbohydrate will point away from the binding site and toward a solvent channel in the crystal, and consequently Asn203 glycosylation will not interfere with Ig2-Ig3 interactions. An interaction between the two Ig3 modules is observed at the interface, as Gln196 makes a water-mediated H-bond with Gln278. The total buried surface of the Ig2-to-Ig3 interface is 1407 Å^2 per dimer. According to Janin (1997), the probability of finding a nonspecific interface of the size of the Ig2-to-Ig3 contact is only 1.9%.

Another antiparallel interaction between two Ig1-2-3 molecules is formed between two Ig2 modules (Figures 2C and 2D). This interaction involves residues 103-121 and 150-158 of the AA′-loop/A′-strand/A′B-loop and the DE-loop/E-strand and has the total buried surface of 958 Å^2 per dimer (Figure 3C). Here, the central residue appears to be Glu114, which makes two H-bonds to Ser151 (side chain and backbone). Apart from an extensive hydrogen-bonding network, especially through water molecules, Val117, Val119, Leu150, and Tyr154 of both Ig2 modules form a number of hydrophobic contacts with each other at the Ig2-to-Ig2 interface (not shown).

A slightly smaller antiparallel interaction (858 Å^2 of total buried surface per dimer) is formed between the Ig1 and Ig3 modules (Figures 2C and 2D), involving residues 32-47 and 76-88 from the C-strand/CC′-loop/C′-strand/C′D-loop and F-strand/FG-loop/G-strand in Ig1, and residues 198, 213-223, and 248-253 from the A-strand, B-strand/BC-loop, and D-strand/DE-loop in Ig3 (Figure 3D). Arg198 and Asp249 form direct H-bonds to the backbone oxygen atoms of Ala81 and Glu82 and two salt bridges with Lys76, respectively. Additionally, one water-mediated H-bond is formed between Lys42 and Asp250, one between Ser44 and Gly220, and two between Ser44 and Glu223. The conserved Phe36 and Phe221 are packed against Asp249 and Gln47, respectively. Together two Ig1-to-Ig3 interaction sites and one Ig2-to-Ig2 site make up a predominant contact between Ig1-2-3 dimers in the crystal (2654 Å^2) forming the second array of Ig1-2-3 dimers (Figures 2C and 2D) perpendicular to the Ig2-to-Ig3-mediated array (Figures 2A and 2B). Contact areas of similar sizes have been found in other CAMs. *Cis* dimers of human ICAM-1 and mouse JAM have 1100 Å^2 and 1200 Å^2 of total buried surface area (per dimer), respectively (Casasnovas et al. 1998; Kostrewa et al., 2001), whereas *trans* dimers of rat CD2 and chicken axonin-1/TAG-1 have even larger contact areas of 1300 Å^2 and 2000 Å^2 (Jones et al., 1992; Freigang et al., 2000).

The Ig3 Module Does Not Dimerize in Solution

The molecular weight of the deglycosylated Ig3 module in solution was determined by DLS to be ~11.2 kDa, which corresponds to a monomer. In agreement with this observation, a small antiparallel contact is formed between two Ig3 modules in the crystal, involving the polar residues 260-264 from the EF-loop with a total buried area of only 487 Å^2 per dimer (not shown). The Ig3-to-Ig3 contact does not involve residues of the previously suggested homophilic binding sequence (Rao et al., 1992), and probably only reflects a crystal packing contact.

Ig3 Inhibits NCAM-Dependent Neurite Outgrowth

NCAM-NCAM interaction is known to induce neurite outgrowth from NCAM-expressing PC12-E2 cells grown on a confluent monolayer of NCAM-expressing fibroblasts (Kolkova et al., 2000). Inhibition of the NCAM-NCAM interaction will therefore inhibit neurite outgrowth in PC12-E2 cells.

In order to examine the biological significance of the observed Ig1-to-Ig3 and Ig2-to-Ig3 contacts in the structure of NCAM Ig1-2-3, we tested the inhibitory effect of the recombinant Ig3 module on NCAM-NCAM adhesion. Furthermore, we prepared two Ig3 mutants containing mutations of the residues R198A, D249G, and E253A (Ig3mut1) of the Ig1-to-Ig3 contact site (see Figure 3D) and K285A, F287A (Ig3mut2) of the Ig2-to-Ig3 contact site (see Figure 3B). In Figure 4 it can be seen that the wild-type Ig3 module (Ig3wt) indeed has an inhibitory effect, whereas both mutants are inactive, thereby strongly supporting that both the Ig1-to-Ig3 and Ig2-to-Ig3 contact sites are participating in homophilic interactions.

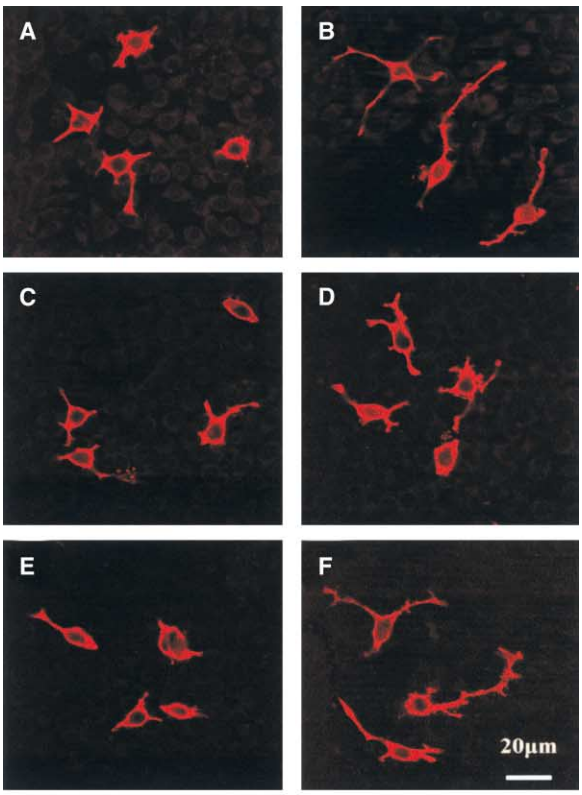

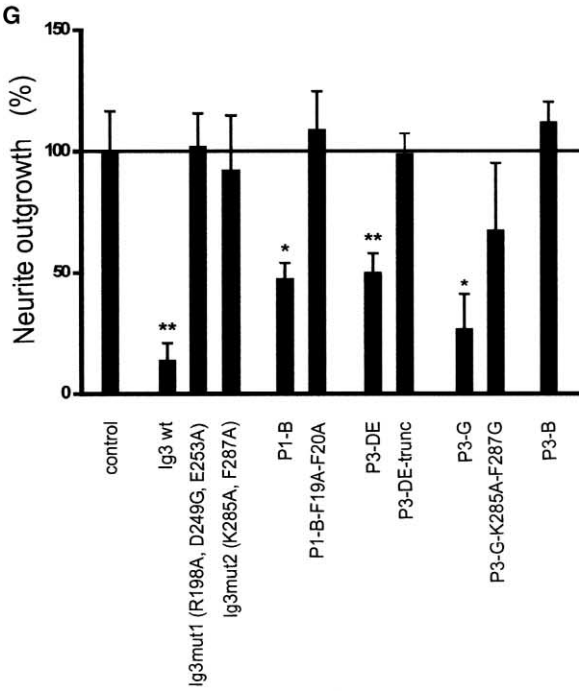

Figure 4. The Effect of the Ig3 Module, the P1-B, P3-DE, P3-G, P3-B Peptides, and Their Derivatives, on Neurite Outgrowth from the NCAM-Expressing PC12-E2 Cells Grown on Top of a Confluent Monolayer of NCAM-Transfected Fibroblasts

(A–F) Confocal micrographs of NCAM-expressing pheochromocytoma PC12-E2 cells grown on top of a confluent monolayer of vector-transfected (A, C, and E) or NCAM-140 transfected (B, D, and F) L929 fibroblasts. NCAM-NCAM interaction stimulates neurite outgrowth in PC12-E2 cells grown on top of NCAM-expressing (B) versus NCAM-negative (A) fibroblasts. Introduction of the recombinant Ig3 module does not affect PC12-E2 cells grown on vector-transfected fibroblasts (C) but clearly inhibits neurite outgrowth in PC12-E2 cells grown on NCAM-transfected fibroblasts (D) as a result of disruption of NCAM-NCAM interactions. In contrast, Ig3mut2 neither affects PC12-E2 cells grown on vector-transfected fibroblasts (E) nor inhibits NCAM-induced neurite outgrowth (F). Peptides P1-B, P3-DE, and P3-G have inhibitory effects comparable to the effect of Ig3wt (C and D), whereas effects of the Ig3mut1, P3-B peptide, and control peptides are similar to the effect of Ig3mut2 (E and F). Scale bar, 20 μm.

(G) The effect of the Ig3 module, P1-B, P3-DE, P3-G, P3-B peptides, and their derivatives, is shown in percent of control, setting the difference between the average neurite length of PC12-E2 cells grown on NCAM-140-transfected and vector-transfected fibroblasts to 100%. Results are given as mean ± SEM.* $P < 0.05$, ** $P < 0.01$ (compared to the induction of neurite outgrowth from PC12-E2 cells grown on top of monolayer of NCAM-transfected fibroblasts).

A similar coculture test-system of NCAM-expressing chicken retinal ganglion cells grown on top of NCAM-140-transfected mouse L cells has been successfully used to demonstrate a disruptive effect of mutations in the Ig3 module homophilic binding site (Ig1-to-Ig3 binding site in the present work) as well as to show an inhibition of neurite outgrowth by synthetic peptides representing this homophilic binding site (Sandig et al., 1994).

Interaction Interface Peptides Inhibit Neurite Outgrowth

It has previously been demonstrated that peptides representing homophilic binding sequences from Ig3 and Ig2 modules of NCAM inhibit NCAM-mediated cell aggregation (Rao et al., 1992, 1994; Sandig et al., 1994; Soroka et al., 2002). Therefore, in order to further examine the biological significance of the observed Ig1-to-Ig2, Ig1-to-Ig3, and Ig2-to-Ig3 contacts in the structure of NCAM Ig1-2-3, we tested the inhibitory effect of a series of peptides representing amino acid sequences from the observed contact areas (Figure 4).

The Ig1-to-Ig2 contact was represented by a peptide 10-GEISVGESKFFL-21 (P1-B), covering the B β-strand of Ig1 and containing the key residue Phe19 in the Ig1-to-Ig2 binding (Kasper et al., 2000; Atkins et al., 2001). As a negative control, the peptide GEISVGESK*aa*L (P1-B-F19A-F20A) containing a double Ala substitution of both Phe19 and Phe20 was used.

The Ig1-to-Ig3 contact was represented by a peptide 244-KHIFSDDSSELTIRNVDKNDE-264 (P3-DE), covering the sequence of the D and E β-strands and the E-F-loop of the Ig3 module. This peptide is homologous to the sequence previously suggested to be a homophilic binding site in the Ig3 module of chicken NCAM (243-KYSFNYDGSELIIKKVDKSDE-263) (Rao et al., 1992). As a negative control, a truncated version of the P3-DE peptide 244-KHIFSDDSSE-253 (P3-DE-trunc) was used. The P3-DE-trunc peptide is homologous to the 243-KYSFNYDGSE-252 chicken sequence that was less potent than the longer sequence (Rao et al., 1992).

The Ig2-to-Ig3 contact was represented by a peptide 281-SIHLKVFAK-289 (P3-G) from the Ig3 module. This

sequence covers the C-terminal part of the G β-strand including the solvent-exposed Phe287. As a negative control, the peptide SIHL*a*V*g*AK (P3-G-K285A-F287G) with substitutions of Lys285 and Phe287 was used. Both P1-B and P3-G peptides contain two hydrophobic residues (Ile and Val/Leu) close to their N termini and at least one Phe residue close to their C termini. As a control peptide with similar hydrophobic properties we selected a peptide 213-TLVADADGFPEP-224 (P3-B) covering the B β-strand and B-C-loop of the Ig3 module, and including Gly220, Phe221, and Glu223 involved in Ig1-to-Ig3 binding. In spite of sequence similarity with P1-B and P3-G peptides, the P3-B peptide was not active (Figure 4G). This is probably due to the fact that Phe221 in Ig3 is partially solvent exposed and Gly220 and Glu223 form water-mediated hydrogen bonds (Figure 3D). In contrast, the peptides P1-B, P3-DE, and P3-G either contain Phe buried in a hydrophobic pocket or residues forming direct H-bonds (Figure 3).

In conclusion, the cell coculture experiments demonstrated that the P1-B, P3-DE, and P3-G peptides all inhibited NCAM-stimulated neurite outgrowth, indicating an impaired NCAM-NCAM binding between the two cell layers. The corresponding control peptides had little or no inhibitory effect (Figure 4G). The P1-B peptide interferes with the Ig1-to-Ig2 interaction and thereby inhibits the Ig1-Ig2-mediated *cis* dimerization of NCAM. In the crystals of the Ig1-2-3 module zipper-like arrays of NCAM *cis* dimers are observed, reflecting *trans* interactions of NCAM. *Trans* interactions therefore seem to require *cis* dimerization of NCAM molecules (Figure 2). The P3-DE and P3-G peptides will not affect *cis* interactions but interfere with *trans* interactions. Since the NCAM-dependent neurite outgrowth relies on NCAM-NCAM interactions between the two cell layers, an inhibition of these interactions will directly affect NCAM-mediated neurite outgrowth.

In our study, we show that mutations in the peptides derived from the Ig3 module produce the same effect as that of the similar mutations in the Ig3 module. This demonstrates that in this experimental setup the employed peptides mimic the Ig3 module, and thus can be used as a convenient and simple tool for further analysis. Moreover, the peptides representing the sequence of the Ig3 module homophilic binding site of chicken NCAM (Ig1-to-Ig3 binding site in the present work) have been previously used to identify and characterize the Ig3 module homophilic binding site (Rao et al., 1992, 1994; Sandig et al., 1994). These results, combined with the Ig3 mutation studies, provide strong evidence for a biological role of the observed Ig1-to-Ig2, Ig1-to-Ig3, and Ig2-to-Ig3 contacts.

Novel Zipper Mechanism for NCAM Homophilic Adhesion

The crystal structure of the Ig1-2-3 fragment reveals novel interactions between the Ig1 and Ig3 and the Ig2 and Ig3 modules of NCAM, as well as showing previously observed Ig1-to-Ig2 and Ig2-to-Ig2 interactions (Kasper et al., 2000). Together, these contacts mediate formation of two perpendicular zipper-like arrays of the Ig1-2-3 dimers (Figure 2). The parallel interaction of the NCAM Ig1-2-3 molecules in the crystal mediated by the Ig1-to-Ig2 contact may reflect an interaction between NCAM molecules present on the same cell surface—*cis* interaction. The antiparallel interactions mediated by the Ig1-to-Ig3, Ig2-to-Ig2, and the Ig2-to-Ig3 contacts may reflect the interaction of NCAM molecules present on opposing cells—*trans* interactions. Based on all presented observations, we propose a model for NCAM homophilic adhesion, consisting of two zipper-like arrays of NCAM molecules (Figure 5). In the "compact" zipper (Figure 5A), NCAM *cis* dimers originating from opposing cell membranes are arranged as arrays through Ig1-to-Ig3 and Ig2-to-Ig2 interactions. We speculate that compact zippers are likely to form first as they allow larger distances between opposing cell membranes than the perpendicular "flat" zippers. In the flat zipper (Figure 5B), the Ig2-to-Ig3 interactions suggest a lateral association between the NCAM compact zippers, thereby forming a double zipper adhesion complex (Figure 5C). The glycosylation at Asn203 of Ig3 (Figure 2) is not likely to interfere with the ability to form the zippers as supported by the fact that the glycosylated Ig3 module inhibits NCAM-mediated neurite outgrowth, whereas glycosylated Ig3mut2 containing mutations at the Ig2-Ig3 binding site is inactive (Figures 4F and 4G). In the compact zipper, the heparin binding sites (133-KHKGRDVILKKDVRFI-148) (Cole and Akeson, 1989) of Ig1-2-3 molecules are solvent exposed (Figures 2C and 2D) and therefore accessible for binding to heparin and heparan sulfate molecules, suggesting that NCAM can be engaged in homophilic and heterophilic interactions simultaneously.

In order to accommodate all seven extracellular modules of NCAM within a typical distance between plasma membranes of ~30 nm (Hall and Rutishauser, 1987), a bend has to be introduced in the NCAM molecules in our model (Figure 5). Analyses of NCAM by electron microscopy have revealed such a bent rod-like structure (Hall and Rutishauser, 1987; Becker et al., 1989). The angle of the bend at the hinge-region between N-terminal (~18 nm) and C-terminal (~10 nm) parts varies considerably (50–140°) with an average value of 98° (Becker et al., 1989) and presumably provides sufficient internal flexibility for NCAM to fit within the cell-cell distance. Based on these studies and on an average length of ~4.3 nm for an Ig module (present work) and ~3.5 nm for a FnIII module (Leahy et al., 1996), the hinge region is most likely located after Ig4. A multiple sequence alignment of NCAM sequences from various species of vertebrates reveals conserved Pro, Lys, and Gly residues in the PKLQGP sequence connecting the Ig4 and Ig5 modules. Since Pro and Gly are typically associated with polypeptide bends, this sequence is likely to introduce a bend between Ig4 and Ig5 modules. The double zipper observed in the crystal (Figure 5C) presents Ig modules 1 to 3 at differing heights, implying that the NCAM molecules upon coexistence of the zippers are bent with different angles. This is in accordance with the electron microscopy data (Hall and Rutishauser, 1987; Becker et al., 1989).

Although *cis* interactions between the Ig1-Ig2 modules do not mediate cell-cell interactions themselves, they probably contribute to the stability of the *trans*

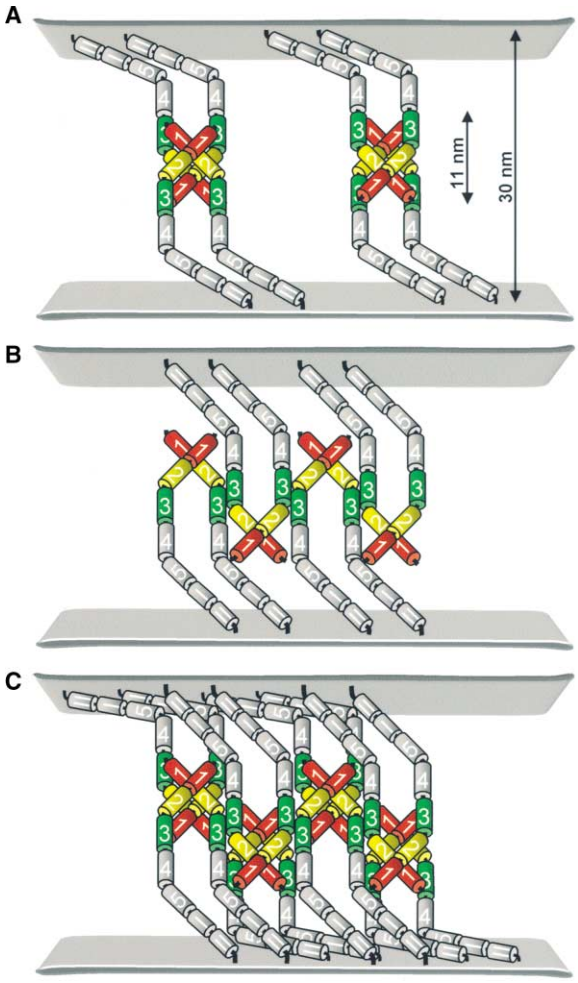

Figure 5. Schematic Representations of the Compact, Flat, and "Double" Zipper Adhesion Complexes Formed by NCAM, as Observed in the Crystal Structure of the NCAM Ig1-2-3 Fragment

The individual Ig modules of Ig1-2-3 are shown as cylinders (Ig1 is red, Ig2 is yellow, and Ig3 is green). The Ig4, Ig5, and the two membrane proximal FnIII modules have been modeled as gray cylinders. Ig and FnIII modules are numbered by Arabic and Roman numerals, respectively. In order to accommodate all seven extracellular modules of NCAM a bend has been introduced after Ig4 according to electron microscopy studies (Hall and Rutishauser, 1987; Becker et al., 1989). The size of the Ig1-2-3 fragment and distance between opposing cell membranes are indicated.

(A) The compact zippers are stabilized by Ig1-to-Ig3 and Ig2-to-Ig2 interactions between Ig1-2-3 *cis* dimers originating from two opposing cell membranes.

(B) The flat zipper is stabilized by Ig2-to-Ig3 interactions between Ig1-2-3 *cis* dimers originating from two opposing cell membranes.

(C) The two types of zippers may coexist as observed in the crystal and will result in formation of a double zipper-like adhesion complex.

interactions. This contention is supported by the cell coculture experiments using the P1-B peptide corresponding to the site in Ig1 binding to Ig2 (Figure 4). Furthermore, an inhibitory effect on cell aggregation was recently demonstrated for a peptide 172-GRILARGEINFK-182 (P2 peptide) representing the site in the Ig2 module binding to the Ig1 module (Soroka et al., 2002). Therefore, we suggest that the formation of *cis* dimers may be a prerequisite for the establishment of *trans* interactions.

To our knowledge, only three X-ray structures of Ig module containing adhesion molecules have been determined comprising three or more Ig modules (axonin-1/TAG1 [Freigang et al., 2000], hemolin [Su et al., 1998], and CD4 [Wu et al., 1997]). A similar zipper-like array of *trans*-interacting *cis* homodimers has been observed in the crystal structure of the junctional adhesion molecule (JAM) (Kostrewa et al., 2001). A zipper-like mechanism of homophilic interactions was also suggested for axonin-1/TAG-1 (Freigang et al., 2000), where molecules alternately provided by opposed membranes form a linear zipper-like array. However, the double zipper formed by NCAM differs fundamentally from the previously described zippers.

In conclusion, we here present a novel model for NCAM homophilic binding that is based on the formation of zippers. The model is in agreement with a number of studies demonstrating that the Ig1, Ig2, and Ig3 modules all are involved in NCAM homophilic binding (Rao et al., 1992; Sandig et al., 1994; Kiselyov et al., 1997; Jensen et al., 1999; Kasper et al., 2000; Atkins et al., 2001) and reconciles a large body of conflicting biological data. The crystal structure of the Ig1-2-3 fragment reveals details of two so far unknown interactions between Ig1 and Ig3 and between Ig2 and Ig3. Interestingly, the Ig1 and Ig2 modules of NCAM mediate both *cis* and *trans* interactions simultaneously, whereas Ig3 is involved only in *trans* interactions. All taken together, our study implies that it is the joined forces of the first three Ig modules that confer the strength of the NCAM-mediated adhesion.

Experimental Procedures

Production of the Ig1-2-3 and Ig3 Fragments of NCAM

The NCAM Ig1-2-3 and Ig3 fragments were produced as recombinant proteins in the yeast *P. pastoris* expression system (Invitrogen). The cDNA fragments encoding Ig1-2-3 and Ig3 of rat NCAM (NCBI accession number NP_113709), corresponding to residues 1-289 and 191-289, respectively, were synthesized by PCR using rat NCAM cDNA as a template. The following DNA primers were used for cloning of Ig1-2-3 and Ig3, respectively: upper (5′-TCTCTCGAGTTC TGCAGGTAGATATTGTT-3′) and lower (5′-AAACCCGGGTTACTTT GCAAAGACCTT-3′), upper (5′-GAATACGTAACTGTCCAGGCCA GAC-3′) and lower (5′-AAACCTAGGTTACTTTGCAAAGACCTTG-3′). The amplified cDNA fragments were subcloned into the pHIL-S1 and the pPIC9K plasmids (Invitrogen), respectively. The recombinant plasmids were linearized with the NsiI and SacI restriction enzymes, respectively, and used for transformation of the *P. pastoris* strain His4 GS-115 (Invitrogen). Large-scale production of the recombinant proteins was performed employing a high-density feed-batch fermentation technique in a Biostat B fermentor (B. Braun Biotech Int. GmbH). Ig1-2-3 and Ig3 were purified from concentrated and desalted medium by anion-exchange chromatography on a HiTrap Q-Sepharose 5 ml column (Pharmacia), followed by gel filtration chromatography on a HiLoad 16/60 Superdex-75 column (Pharmacia). The Ig1-2-3 was enzymatically deglycosylated with PNGase-F endo-N-glycosidase (New England Biolabs) at 37°C in PBS buffer (pH 7.4). The authenticity of the protein fragments was confirmed by DNA sequencing of the recombinant plasmids, by amino acid sequencing of the 10-12 N-terminal residues, and by MALDI-TOF MS. The recombinant Ig1-2-3 and Ig3 fragments contained, respectively, two (RV) and five (EAEAY) additional N-terminal residues from the cloning vector. The purity of the proteins was at least 95% as estimated by SDS-PAGE.

Production of the Ig1-2-3 and Ig3 Mutants

An Ig1-2-3 mutant (Ig1-2-3mut) containing the substitutions E11A, E16A, and K18A was produced as a recombinant protein in the yeast *P. pastoris* expression system following the procedure described for the Ig1-2-3 fragment. The three mutations were introduced by PCR using the following DNA primer: upper (5′-CTGCAGGTAGATATTGT TCCCAGCCAAGGAGCCATCAGCGTTGGAGCCTCCGCCTTCTTCC TGTGTCAAGTGGCA-3′).

Two Ig3 mutants containing the substitutions R198A, D249G, E253A (Ig3mut1), and K285A, F287A (Ig3mut2) were produced as recombinant proteins in the yeast *P. pastoris* expression system following the procedure described for the Ig3 fragment. Mutations were introduced by PCR using the following DNA primers: upper1 (5′-AAATACGTAACTGTCCAGGCCGCCCAGAGCATCGTG-3′), upper2 (5′-GGCGACAGTTCGGCGTTA ACCATCAGGAATGTGGAC-3′), and lower (5′-GGTTAACGCCGAACTGTCGCCACTGAAGATGTGCT TCTC-3′) for Ig3mut1, and lower (5′-AAACTTAGGTTACTTTGCTGC GACTGCGAGGTGGATGGAGGC ATC-3′) for Ig3mut2. The DNA constructs of Ig1-2-3mut, Ig3mut1, and Ig3mut2 were verified by DNA sequencing. Folding of the Ig3 module and its mutants, as well as presence of carbohydrates, was confirmed by one-dimensional proton NMR spectra recorded at 800 MHz on a Varian NMR spectrometer (Varian, Inc.) at 25°C in PBS buffer (pH 7.4).

Preparation of Peptides

Peptides were synthesized using the 9-fluorenylmethoxycarbonyl (Fmoc) protection strategy on a TentaGel resin (Rapp Polymere) using Fmoc protected amino acids (Calbiochem-Novabiochem). Peptides were at least 85% pure as estimated by MALDI-TOF MS. All peptides were synthesized with free NH_2 and carboxy-amidated COOH groups.

Crystallization and Data Collection

Crystals of NCAM Ig1-2-3 were grown at 18°C using the hanging-drop vapor diffusion method, with drops of equal volumes of reservoir and protein solutions (4 mg ml^{-1} in 5 mM Na phosphate, 150 mM NaCl [pH 7.4]). The reservoir solution contained 14%–17% w/v PEG 4000, 450 mM Li sulfate, and 100 mM Na acetate (pH 5.2). The crystals belong to space group $I2_12_12_1$ with one molecule in the asymmetric unit and cell dimensions of a = 51.5, b = 108.5, and c = 149.0 Å. The crystals were flash cooled in liquid nitrogen using 15% v/v glycerol as cryoprotectant. Two data sets were collected on the same crystal. The high-resolution data were collected to 2.0 Å at 120 K at beamline I711, Max-Lab, Lund, Sweden, and the low-resolution data were collected to 3.5 Å at 120 K on a Rigaku RU300 rotating anode equipped with a MAR345 image plate detector. The data sets were combined and processed with DENZO/SCALEPACK (Otwinowski and Minor, 1997) and the CCP4 suite of programs (CCP4, 1994).

Structure Determination and Refinement

The structure was determined by molecular replacement with the programs AmoRe (Navaza and Saludjian, 1997) and CNS version 1.0 (Brünger et al., 1998), using the X-ray structures of the Ig2 and Ig1 modules of NCAM (Kasper et al., 2000) as search models. Initially, the position of the Ig2 module was located using AmoRe. The Ig1 module was subsequently located using CNS. An electron density map was calculated based on phase information from Ig1 and Ig2. Residues of Ig3 were gradually built into this map. Map interpretation and model building were carried out using the program O (Jones et al., 1991). After several building and refinement cycles, ARP/wARP version 5.1 (Perrakis et al., 1999) was used to rebuild 233 out of 291 residues of NCAM Ig1-2-3. CNS was used to carry out the final rounds of refinements. The final model contains amino acids (-1)-238 and 241-289 and 265 water molecules. Amino acids are numbered according to the mature sequence of NCAM. Residues Arg and Val originating from the cloning site were given negative integers -2 and -1, respectively. Using all reflections in the resolution range 50-2.0 Å, the R_{cryst} is 21.8% and the R_{free} is 23.8% (3% test set, corresponding to 828 reflections). Data collection and refinement statistics are given in Table 1. Interdomain geometry was determined according to Bork et al. (1996), and buried accessible surface areas were calculated using the Protein-Protein Interaction Server (http://www.biochem.ucl.ac.uk/bsm/PP/server) (Jones and Thornton, 1996). Figures were prepared with the programs MOLSCRIPT, RASTER3D (Kraulis, 1991; Merritt and Bacon, 1997), and Insight II (Accelrys).

Cell Culture and Immunostaining

The NCAM-expressing pheochromocytoma PC12-E2 cell line (Wu and Bradshaw, 1995) was a gift from Dr. Klaus Seedorf, Hagedorn Research Institute, Denmark. The cells were grown in Dulbecco's Modified Eagle's Medium (DMEM) supplemented with 5% v/v fetal calf serum (FCS) and 10% v/v horse serum (HS), 100 U ml^{-1} penicillin, 100 μg ml^{-1} streptomycin (all from Gibco BRL) at 37°C in a humidified atmosphere containing 5% CO_2. The fibroblastoid mouse cell line, L929 (European Cell Culture Collection), was stably transfected with the eukaryotic expression vector pHβ-Apr-1-neo (Gunning et al., 1987) containing a full-length cDNA encoding human 140 kDa NCAM-B or the vector alone. The NCAM cDNA did not contain the exons VASE, a, b, c, or AAG. The cells were routinely grown at 37°C, 5% CO_2 in DMEM supplemented with 10% v/v FCS, 100 U ml^{-1} penicillin, and 100 μg ml^{-1} streptomycin. For analysis of neurite outgrowth, PC12-E2 cells (8,000 cells per well) were seeded on top of a confluent monolayer of transfected fibroblastoid L929 cells in four-well LabTek Tissue Culture Chamber Slides (NUNC). The cells were grown for 24 hr in DMEM supplemented with 1% v/v HS, before analysis. The glycosylated recombinant rat Ig3 module of NCAM (wild-type and mutated forms) or selected peptides were added immediately after seeding of PC12-E2 cells in order to evaluate their inhibitory effects on adhesion, as reflected by interference with NCAM-mediated neurite outgrowth. Ig3wt, Ig3mut1, and Ig3mut2 were tested at a concentration of 500 μg ml^{-1}. All peptides were tested at a concentration of 200 μg ml^{-1}. Proper controls were included and the person performing the experiments did not know the identity of the mutants or peptides.

To evaluate the length of processes of PC12-E2 cells, the cocultures were fixed in 4% w/v paraformaldehyde for 25 min. After washing in PBS, cells were blocked with 10% v/v goat serum (DAKO) for 30 min and subsequently incubated for 1 hr at room temperature with a mouse monoclonal anti-Thy-1 antibody (Caltag Laboratories) (1:100 in PBS containing 10% v/v goat serum). After washing, cells were incubated for 1 hr at room temperature with Alexa-Fluor 568 goat anti-mouse IgG (Molecular Probes) (1:1000 in PBS containing 10% goat serum). All washes were performed for 10 min in PBS and repeated three times.

The total neurite length per cell was analyzed using the software ProcessLength (Rønn et al., 2000). Five independent experiments with the Ig3 module, its mutants, and the individual peptides were performed. In each experiment neurites from 200–300 cells were analyzed. In order to compare results of individual experiments and due to the inherently high variability of cell experiments, the data were normalized, setting the difference between the average neurite length of PC12-E2 cells grown on NCAM-140-transfected and vector-transfected fibroblasts to 100%. Statistical evaluations were performed using a two-sided Student's *t*-test.

Dynamic Light Scattering Measurements

Measurements were performed using a DynaPro-MS/X instrument (Protein Solutions) at 18°C. The deglycosylated preparations of Ig1-2-3 (4 mg ml^{-1}), Ig1-2-3mut (4 mg ml^{-1}), and Ig3 (10 mg ml^{-1}) in PBS (pH 7.4) were used to determine the molecular weight of the recombinant proteins in solution.

Acknowledgments

We thank Dr. Yngve Cerenius and Dr. Jörg Freigang for expert technical assistance during data collection. This work was supported by grants from the Lundbeck Foundation, the Danish Medical Research Council, the Danish Cancer Society, DANSYNC (Danish Center for Synchrotron Based Research), Novo Nordisk Fonden, Apotekerfonden of 1991, the Carlsberg Foundation, the John and Birthe Meyer Foundation, the European Union program (Age-Related Changes in Learning and Memory), and the European Community (Access to Research Infrastructure Action of the Improving Human Potential Programme) to the EMBL Hamburg Outstation.

Received: June 3, 2003
Accepted: June 11, 2003
Published: September 30, 2003

References

Atkins, A.R., Osborne, M.J., Lashuel, H.A., Edelman, G.M., Wright, P.E., Cunningham, B.A., and Dyson, H.J. (1999). Association between the first two immunoglobulin-like domains of the neural cell adhesion molecule N-CAM. FEBS Lett. *451*, 162–168.

Atkins, A.R., Chung, J., Deechongkit, S., Little, E.B., Edelman, G.M., Wright, P.E., Cunningham, B.A., and Dyson, H.J. (2001). Solution structure of the third immunoglobulin domain of the neural cell adhesion molecule N-CAM: can solution studies define the mechanism of homophilic binding? J. Mol. Biol. *311*, 161–172.

Becker, J.W., Erickson, H.P., Hoffman, S., Cunningham, B.A., and Edelman, G.M. (1989). Topology of cell adhesion molecules. Proc. Natl. Acad. Sci. USA *86*, 1088–1092.

Berezin, V., Bock, E., and Poulsen, F.M. (2000). The neural cell adhesion molecule. Curr. Opin. Drug Discov. Dev. *3*, 605–609.

Bork, P., Downing, A.K., Kieffer, B., and Campbell, I.D. (1996). Structure and distribution of modules in extracellular proteins. Q. Rev. Biophys. *29*, 119–167.

Brieher, W.M., Yap, A.S., and Gumbiner, B.M. (1996). Lateral dimerization is required for the homophilic binding activity of C-cadherin. J. Cell Biol. *135*, 487–496.

Brünger, A.T., Adams, P.A., Clore, G.M., DeLano, W.L., Gros, P., Grosse-Kunstleve, R.W., Jiang, J.-S., Kuszewski, J., Nilges, M., Pannu, N.S., et al. (1998). Crystallography & NMR system: a new software suite for macromolecular structure determination. Acta Crystallogr. D *54*, 905–921.

Casasnovas, J.M., Stehle, T., Liu, J.H., Wang, J.H., and Springer, T.A. (1998). A dimeric crystal structure for the N-terminal two domains of intercellular adhesion molecule-1. Proc. Natl. Acad. Sci. USA *95*, 4134–4139.

Chothia, C., and Jones, E.Y. (1997). The molecular structure of cell adhesion molecules. Annu. Rev. Biochem. *66*, 823–862.

Cole, G.J., and Akeson, R. (1989). Identification of a heparin binding domain of the neural cell adhesion molecule N-CAM using synthetic peptides. Neuron *2*, 1157–1165.

CCP4 (Collaborative Computational Project 4) (1994). The CCP4 suite: programs for protein crystallography. Acta Crystallogr. D *50*, 760–763.

Covault, J., and Sanes, J.R. (1985). Neural cell adhesion molecule (NCAM) accumulates in denervated and paralyzed skeletal muscles. Proc. Natl. Acad. Sci. USA *82*, 4544–4548.

Cunningham, B.A., Hemperly, J.J., Murray, B.A., Prediger, E.A., Brackenbury, R., and Edelman, G.M. (1987). Neural cell adhesion molecule: structure, immunoglobulin-like domains, cell surface modulation, and alternative RNA splicing. Science *236*, 799–806.

Flocco, M.M., and Mowbray, S.L. (1994). Planar stacking interactions of arginine and aromatic side-chains in proteins. J. Mol. Biol. *235*, 709–717.

Freigang, J., Proba, K., Leder, L., Diederichs, K., Sonderegger, P., and Welte, W. (2000). The crystal structure of the ligand binding module of axonin-1/TAG-1 suggests a zipper mechanism for neural cell adhesion. Cell *101*, 425–433.

Gunning, P., Leavitt, J., Muscat, G., Ng, S.Y., and Kedes, L. (1987). A human beta-actin expression vector system directs high-level accumulation of antisense transcripts. Proc. Natl. Acad. Sci. USA *84*, 4831–4835.

Hall, A.K., and Rutishauser, U. (1987). Visualization of neural cell adhesion molecule by electron microscopy. J. Cell Biol. *104*, 1579–1586.

Hunter, I., Sawa, H., Edlund, M., and Öbrink, B. (1996). Evidence for regulated dimerization of cell-cell adhesion molecule (C-CAM) in epithelial cells. Biochem. J. *320*, 847–853.

Janin, J. (1997). Specific versus non-specific contacts in protein crystals. Nat. Struct. Biol. *4*, 973–974.

Jensen, P.H., Soroka, V., Thomsen, N.K., Ralets, I., Berezin, V., Bock, E., and Poulsen, F.M. (1999). Structure and interactions of NCAM modules 1 and 2 - basic elements in neural cell adhesion. Nat. Struct. Biol. *6*, 486–493.

Jones, S., and Thornton, J.M. (1996). Principles of protein-protein interactions. Proc. Natl. Acad. Sci. USA *93*, 13–20.

Jones, T.A., Zou, J.Y., Cowan, S.W., and Kjeldgaard, M. (1991). Improved methods for building protein models in electron density maps and the location of errors in these models. Acta Crystallogr. A *47*, 110–119.

Jones, E.Y., Davis, S.J., Williams, A.F., Harlos, K., and Stuart, D.I. (1992). Crystal structure at 2.8 A resolution of a soluble form of the cell adhesion molecule CD2. Nature *360*, 232–239.

Kallapur, S.G., and Akeson, R.A. (1992). The neural cell adhesion molecule (NCAM) heparin binding domain binds to cell surface heparan sulfate proteoglycans. J. Neurosci. Res. *33*, 538–548.

Kasper, C., Stahlhut, M., Berezin, V., Maar, T.E., Edvardsen, K., Kiselyov, V.V., Soroka, V., and Bock, E. (1996). Functional characterization of NCAM fibronectin type III domains: demonstration of modulatory effects of the proline-rich sequence encoded by alternatively spliced exons a and AAG. J. Neurosci. Res. *46*, 173–186.

Kasper, C., Rasmussen, H., Kastrup, J.S., Ikemizu, S., Jones, E.Y., Berezin, V., Bock, E., and Larsen, I.K. (2000). Structural basis of cell-cell adhesion by NCAM. Nat. Struct. Biol. *7*, 389–393.

Kiselyov, V.V., Berezin, V., Maar, T., Soroka, V., Edvardsen, K., Schousboe, A., and Bock, E. (1997). The first Ig-like NCAM domain is involved in both double reciprocal interaction with the second Ig-like NCAM domain and in heparin binding. J. Biol. Chem. *272*, 10125–10134.

Kleywegt, G.J., and Jones, T.A. (1996). Phi/psi-chology: Ramachandran revisited. Structure *4*, 1395–1400.

Kolkova, K., Novitskaya, V., Pedersen, N., Berezin, V., and Bock, E. (2000). Neural cell adhesion molecule-stimulated neurite outgrowth depends on activation of protein kinase C and the Ras-mitogen-activated protein kinase pathway. J. Neurosci. *20*, 2238–2246.

Kostrewa, D., Brockhaus, M., D'Arcy, A., Dale, G.E., Nelboeck, P., Schmid, G., Mueller, F., Bazzoni, G., Dejana, E., Bartfai, T., et al. (2001). X-ray structure of junctional adhesion molecule: structural basis for homophilic adhesion via a novel dimerization motif. EMBO J. *20*, 4391–4398.

Kraulis, P.J. (1991). MOLSCRIPT: a program to produce both detailed and schematic plots of protein structures. J. Appl. Crystallogr. *24*, 946–950.

Leahy, D.J., Aukhil, I., and Erickson, H.P. (1996). 2.0 A crystal structure of a four-domain segment of human fibronectin encompassing the RGD loop and synergy region. Cell *84*, 155–164.

Merritt, E.A., and Bacon, D.J. (1997). Raster3D photorealistic molecular graphics. Methods Enzymol. *277*, 505–524.

Milev, P., Friedlander, D.R., Sakurai, T., Karthikeyan, L., Flad, M., Margolis, R.K., Grummet, M., and Margolis, R.U. (1994). Interactions of the chondroitin sulfate proteoglycan phosphacan, the extracellular domain of a receptor-type protein tyrosine phosphatase, with neurons, glia, and neural cell adhesion molecules. J. Cell Biol. *121*, 1409–1421.

Miyahara, M., Nakanishi, H., Takahashi, K., Satoh-Horikawa, K., Tachibana, K., and Takai, Y. (2000). Interaction of nectin with afadin is necessary for its clustering at cell-cell contact sites but not for its cis dimerization or trans interactions. J. Biol. Chem. *275*, 613–618.

Navaza, J., and Saludjian, P. (1997). AmoRe: an automated molecular replacement program package. Methods Enzymol. *276*, 581–594.

Nybroe, O., Moran, N., and Bock, E. (1989). Equilibrium binding analysis of neural cell adhesion molecule binding to heparin. J. Neurochem. *52*, 1947–1949.

Otwinowski, Z., and Minor, W. (1997). Processing of X-ray diffraction data collected in oscillation mode. Methods Enzymol. *276*, 307–326.

Perrakis, A., Morris, R., and Lamzin, V.S. (1999). Automated protein model building combined with iterative structure refinement. Nat. Struct. Biol. *6*, 458–463.

Probstmeier, R., Kuhn, K., and Schachner, M. (1989). Binding properties of the neural cell adhesion molecule to different components of the extracellular matrix. J. Neurochem. *53*, 1794–1801.

Ranheim, T.S., Edelman, G.M., and Cunningham, B.A. (1996). Homophilic adhesion mediated by the neural cell adhesion molecule involves multiple immunoglobulin domains. Proc. Natl. Acad. Sci. USA *93*, 4071–4075.

Rao, Y., Wu, X.-F., Gariepy, J., Rutishauser, U., and Siu, C.-H. (1992). Identification of a peptide sequence involved in homophilic binding in the neural cell adhesion molecule NCAM. J. Cell Biol. *118*, 937–949.

Rao, Y., Zhao, X., and Siu, C.-H. (1994). Mechanisms of homophilic binding mediated by the neural cell adhesion molecule NCAM. Evidence for isologous interaction. J. Biol. Chem. *269*, 27540–27548.

Rønn, L.C., Ralets, I., Hartz, B.P., Bech, M., Berezin, A., Berezin, V., Moller, A., and Bock, E. (2000). A simple procedure for quantification of neurite outgrowth based on stereological principles. J. Neurosci. Meth. *100*, 25–32.

Sandig, M., Rao, Y., and Siu, C.-H. (1994). The homophilic binding site of the neural cell adhesion molecule NCAM is directly involved in promoting neurite outgrowth from cultured neural retinal cells. J. Biol. Chem. *269*, 14841–14848.

Shapiro, L., Fannon, A.M., Kwong, P.D., Thompson, A., Lehmann, M.S., Grubel, G., Legrand, J.-F., Als-Nielsen, J., Colman, D.R., and Hendrickson, W.A. (1995). Structural basis of cell-cell adhesion by cadherins. Nature *374*, 327–337.

Soroka, V., Kiryushko, D., Novitskaya, V., Rønn, L.C., Poulsen, F.M., Holm, A., Bock, E., and Berezin, V. (2002). Induction of neuronal differentiation by a peptide corresponding to the homophilic binding site of the second Ig module of NCAM. J. Biol. Chem. *227*, 24676–24683.

Su, X.-D., Gastinel, L.N., Vaughn, D.E., Faye, I., Poon, P., and Bjorkman, P.J. (1998). Crystal structure of hemolin: a horseshoe shape with implications for homophilic adhesion. Science *281*, 991–995.

Takeda, H., Shimoyama, Y., Nagafuchi, A., and Hirohashi, S. (1999). E-cadherin functions as a cis-dimer at the cell-cell adhesive interface in vivo. Nat. Struct. Biol. *6*, 310–312.

Tomasiewicz, H., Ono, K., Yee, D., Thompson, C., Goridis, C., Rutishauser, U., and Magnuson, T. (1993). Genetic deletion of a neural cell adhesion molecule variant (NCAM-180) produces defects in the central nervous system. Neuron *11*, 1163–1174.

Wu, Y.Y., and Bradshaw, R.A. (1995). PC12–E2 cells: a stable variant with altered responses to growth factor stimulation. J. Cell. Physiol. *164*, 522–532.

Wu, H., Kwong, P.D., and Hendrickson, W.A. (1997). Dimeric association and segmental variability in the structure of human CD4. Nature *387*, 527–530.

Accession Numbers

The coordinates of the structure have been deposited with the Protein Data Bank under ID code 1QZ1.